

## ***Hydrologic connectivity constrains partitioning of global terrestrial water fluxes***

The Faculty of Oregon State University has made this article openly available.  
Please share how this access benefits you. Your story matters.

<b>Citation</b>	Good, S. P., Noone, D., & Bowen, G. (2015). Hydrologic connectivity constrains partitioning of global terrestrial water fluxes. <i>Science</i> , 349(6244), 175-177. doi:10.1126/science.aaa5931
<b>DOI</b>	10.1126/science.aaa5931
<b>Publisher</b>	American Association for the Advancement of Science
<b>Version</b>	Accepted Manuscript
<b>Terms of Use</b>	<a href="http://cdss.library.oregonstate.edu/sa-termsfuse">http://cdss.library.oregonstate.edu/sa-termsfuse</a>

## **Title: Hydrologic connectivity constrains partitioning of global terrestrial water fluxes**

**Authors:** Stephen P. Good<sup>1,2\*</sup>, David Noone<sup>3</sup>, Gabriel Bowen<sup>1,4</sup>

### **Affiliations:**

<sup>1</sup>Department of Geology and Geophysics, University of Utah, Salt Lake City, UT.

<sup>2</sup>Department of Biological and Ecological Engineering, Oregon State University, Corvallis, OR.

<sup>3</sup>College of Earth, Ocean and Atmospheric Sciences, Oregon State University, Corvallis, OR.

<sup>4</sup>Global Change and Sustainability Center, University of Utah, Salt Lake City, UT.

\*Correspondence to: stephen.good@oregonstate.edu

**Abstract:** Continental precipitation not routed to the oceans as runoff returns to the atmosphere as evapotranspiration. Partitioning this evapotranspiration flux into interception, transpiration, soil evaporation, and surface water evaporation is difficult using traditional hydrological methods yet critical for understanding the water cycle and linked ecological processes. We combined two large-scale flux-partitioning approaches to quantify evapotranspiration sub-components and the hydrologic connectivity of bound, plant-available soil waters with more mobile surface waters. Globally, transpiration is  $64 \pm 13\%$  (mean  $\pm 1$  s.d.) of evapotranspiration, and  $65 \pm 26\%$  of evaporation originates from soils and not surface waters. We estimate  $38 \pm 28\%$  of surface water is derived from the plant-accessed soil water pool. This limited connectivity between soil and surface waters fundamentally structures the physical and biogeochemical interactions of water transiting through catchments.

**One Sentence Summary:** Globally,  $\sim 64\%$  of continental evapotranspiration consists of transpiration and  $\sim 65\%$  of continental evaporation occurs from soils.

**Main Text:** Continental precipitation is routed through soils, plants, and streams on its return to the oceans or atmosphere. This hydrologic routing within catchments determines peak and baseflow stream discharge, plant productivity, and surface water quality. Over the long-term, changes in water storage are minimal and precipitation entering catchments exits as either runoff or evapotranspiration (1). Further partitioning evapotranspiration flux into evaporation and transpiration sub-components is essential for understanding links between ecologic and hydrologic systems because biologic water use is inexorably coupled with ecosystem productivity (2).

At plot scales, transpiration and evaporation fluxes can be directly measured by hydrometric devices such as lysimeters, leaf cuvettes, and sap flow probes, yet these techniques remain difficult to implement at watershed, regional or continental scales (3–6). The classic hydrologic paradigm of transitory flow links these fluxes and posits that infiltration entering the soil column, where it may be used by vegetation, displaces previously held water deeper into the profile and eventually into streams (7). Observed preferential flow paths at hillslope scales (8, 9) and geochemical evidence (10, 11) point to the possibility that soil water used by plants remains separated from water rapidly passing through soils and into open channels. If this hydrologic

separation is established as a generalized phenomena across catchments, models may require a more complex representation of water movement and associated soil biogeochemistry (12).

Two distinct stable isotope techniques have emerged as solutions for flux partitioning at regional to global scales (5). Both approaches leverage differences between the ratio of heavy to light isotopes of water (e.g D/H) in transpiration, which is often assumed un-changed relative to soil source waters (13), and evaporation, which is D-depleted relative to source waters due to the lower vapor pressure and diffusivity of the rare isotopologue (14). Runoff-based techniques use differences in the isotope ratios of precipitation inputs and outflowing runoff from hydrologic basins to partition evapotranspiration, with larger differences indicating more evaporation from surface waters (3, 15, 16). Evapotranspiration-based techniques involve directly measuring the isotopic ratio of upward vapor flux over a region and comparing it to estimated values for the evaporation and transpiration flux end-members (17–19). Though useful, both approaches suffer from key deficiencies. Runoff techniques are unable to consider partial evaporation of soil waters before plant uptake if the remaining water is not discharged to surface waters (20, 21). In contrast evapotranspiration techniques provide information only within the measurement's flux footprint, and results are difficult to extrapolate across regions of heterogeneous surface cover or to areas with open surface water, which typically lie beyond the footprint of conventional flux monitoring stations.

Here, we establish a unified framework for hydrologic partitioning that reconciles runoff and evapotranspiration isotope approaches by quantifying the connectivity between soil matrix waters and mobile surface waters. This 'hydrologic connectivity' is formally defined as the fraction of mobile surface water derived from bound waters (water that resides in the soil matrix and is available to support plant transpiration) as opposed to mobile waters (water that rapidly bypasses soils via preferential flow paths and does not mix with bound waters) (22). In a fully connected system, consistent with the translatory flow paradigm, water accessible to plants and subjected to soil evaporation also moves into streams. In a disconnected system characterized by preferential flow, soil waters do not interact with surface waters and therefore water entering streams and rivers has an isotopic composition equivalent to that of rainfall. This theoretical framework can be applied, using established models for isotopic fractionation and data on isotopic inputs (precipitation) and outputs (runoff, evapotranspiration), to constrain the partitioning of hydrologic fluxes into the sub-components of transpiration, evaporation of bound water in soils, and evaporation from mobile surface waters.

We recently determined the D/H isotope ratios of continental runoff and evapotranspiration (23), independent of terrestrial hydrologic partitioning, via an isotopic mass balance of the oceans and atmosphere. This ocean-atmosphere approach used satellite retrievals of marine surface level D/H isotope ratios in water vapor (24) to estimate oceanic evaporation isotope ratios. Combining these with over-ocean precipitation isotope ratios modeled based on monitoring station data (25), we calculated the isotope ratios of continental fluxes as the residuals of each isotopologue mass balance. Here, over-land precipitation isotope ratios (25) are combined with bulk land-atmosphere water fluxes in gridded simulations of all terrestrial flux sub-components and their isotope ratios to calculate the global terrestrial water isotope budget (22). In determining this budget, the fluxes of soil evaporation, surface water evaporation and hydrologic connectivity are found such that the isotope ratios of continental runoff and evapotranspiration fluxes are consistent with the ocean-atmosphere mass balance (23).

When implementing this framework, constraints on possible runoff, interception, transpiration, and evaporation fluxes within the terrestrial hydrologic cycle (e.g., transpiration may not exceed evapotranspiration) limit the range of continental output flux isotope ratios relative to the previous ocean-atmosphere study (Fig 1A). For global runoff isotope values the revised results are within the range of observed large river values (23). Few direct observations of evapotranspiration isotope values are available for comparison with our result, and large uncertainties persist in accurately measuring this flux (5, 26). Our simulations show that if the value of global runoff is more D-enriched, less transpiration and more surface water evaporation are required to balance the global isotope budget (Fig 1B). Conversely, if the isotopic value of global evapotranspiration is more D-enriched, more transpiration and soil evaporation are required to meet observational constraints (Fig 1D). Overall, the fraction of evaporation occurring in soils is more sensitive to runoff and evapotranspiration composition than is the transpired fraction.

Globally, the transpired fraction of evapotranspiration is estimated to be 56-74% (25<sup>th</sup> to 75<sup>th</sup> percentiles) with a median of 65% and mean of 64%. A previous estimate of global partitioning (3), which did not incorporate evaporation of bound soil water and its connectivity to mobile water, suggested a value of 80-90%. Subsequent critiques and revisions of that study have obtained estimates similar to those reported here, though with greater uncertainty (6, 20). The estimated transpired fraction described here is relatively insensitive to the hydrologic connectivity, which reflects the strong constraint imposed by the high isotope value of global evapotranspiration on the magnitude of this relatively D-enriched flux. We find that the global fraction of evaporation occurring in soils is 45-88%, with a median of 71% and a mean of 65%. Based on our simulations, we estimate hydrologic connectivity to be 14-59%, with a median of 31% and mean of 38%, which suggests a pervasive disconnect between water bound in soils and water entering streams, though not complete separation.

Although local runoff D/H ratios are typically larger than local precipitation D/H ratios, the flux weighted D/H ratio of global runoff is smaller than that of global continental precipitation because of spatial patterns in continental precipitation D/H composition and hydrologic routing. Locally, evaporation of bound soil waters raises the isotope value of transpiration flux because plant roots will withdraw D-enriched soil waters. The skewed distribution of simulation results toward low hydrologic connectivity reflects the fact that at lower connectivity values the flux entering surface waters has smaller D/H ratios because more water is bypassing soils that are D-enriched. Thus, simulations with substantial soil evaporation are consistent with a global evapotranspiration flux that is enriched in D relative to precipitation and simulations with low connectivity are consistent with a global runoff flux that is more depleted in D than precipitation. In contrast to transpired fraction, the bound-water evaporation percentage is weakly correlated with connectivity (Fig 2). This suggests predictive limits of our approach, in that more connected systems with more soil evaporation and less connected systems with less soil evaporation will produce similar continental output flux isotope ratios.

The terrestrial hydrologic partitioning estimated here corresponds to a total transpiration of  $55 \pm 12 \text{ } 10^3 \text{ km}^3 \text{ year}^{-1}$  (mean  $\pm$  1 s.d.), a total soil evaporation of  $5 \pm 4 \text{ } 10^3 \text{ km}^3 \text{ year}^{-1}$ , and a total surface water evaporation of  $2 \pm 2 \text{ } 10^3 \text{ km}^3 \text{ year}^{-1}$ , assuming an interception of  $23 \pm 10 \text{ } 10^3 \text{ km}^3 \text{ year}^{-1}$  (27) and a continental precipitation of  $115 \pm 2 \text{ } 10^3 \text{ km}^3 \text{ year}^{-1}$  (28) (Fig 3). The transpired fraction determined here is consistent with previous meta-analyses (Fig. 1C) and places an observational constraint on transpiration estimates from global Earth system models, which range between

38% and 80% (4–6, 29). The fraction of total evapotranspiration flux occurring from surface waters, 2.9%, is also consistent with values from global Earth System Models, which range from 2 to 4% when reported (29). Globally, tropical forests provide the bulk of continental transpiration, though these regions contribute modest amounts of soil and surface water evaporation as well.

Transpiration fluxes form the primary link between the water and carbon cycles, with water lost from plant stomata during carbon assimilation (i.e. plant water use efficiency) a critical factor determining ecosystem function and productivity. Although we estimate that plant transpiration is a majority of the evapotranspiration flux, our results demonstrate that previous partitioning approaches may overestimate the contribution of transpiration, likely because they do not consider evaporation from multiple catchment water pools and their connectivity. Furthermore, isotopic partitioning approaches are sensitive to bulk fluxes estimates and their uncertainties as well as assumptions about interception rates, with larger interception isotopically indistinguishable from increased transpiration because both fluxes are often assumed unfractionated relative to their source waters (6, 20). Because a majority of evaporation occurs from soils and not open waters more knowledge is needed of the role of ecosystem structure and micro-climate in determining sub-canopy evaporation rates.

Finally, the partial hydrologic disconnect between bound and mobile waters, which our estimates suggest is substantial and pervasive at the global scale, has implications for prediction and monitoring of both water quantity and quality within streams and rivers. The hydrologic and hydrochemical properties of surface water systems are strongly influenced by physical flow paths within the near surface, and the low connectivity found here suggests, for example, that stream biogeochemistry may be less sensitive to soil zone processes than it would be if hydrologic connectivity were higher. Although we determine a single average connectivity value, connectivity varies with geography and in time as preferential flow paths are activated and deactivated throughout the year (30). Indeed, the relation between the connectivity metric and soil-water transit time distributions is likely complex. Given the ubiquitous nature of both water quantity and water quality issues affecting watersheds worldwide, an improved understanding of hydrologic connectivity at variety of temporal and spatial scales is essential.

## References and Notes:

1. T. H. Syed, J. S. Famiglietti, D. P. Chambers, J. K. Willis, K. Hilburn, Satellite-based global-ocean mass balance estimates of interannual variability and emerging trends in continental freshwater discharge. *Proc. Natl. Acad. Sci. U. S. A.* **107**, 17916–21 (2010).
2. B. D. Newman *et al.*, Ecohydrology of water-limited environments: a scientific vision. *Water Resour. Res.* **42**, W06302 (2006).
3. S. Jasechko *et al.*, Terrestrial water fluxes dominated by transpiration. *Nature*. **496**, 347–50 (2013).
4. L. Wang, S. P. Good, K. K. Caylor, Global synthesis of vegetation control on evapotranspiration partitioning. *Geophys. Res. Lett.* **41**, 6753–6757 (2014).
5. S. J. Sutanto *et al.*, HESS Opinions: A perspective on different approaches to determine the contribution of transpiration to the surface moisture fluxes. *Hydrol. Earth Syst. Sci. Discuss.* **11**, 2583–2612 (2014).
6. W. H. Schlesinger, S. Jasechko, Transpiration in the global water cycle. *Agric. For. Meteorol.* **189-190**, 115–117 (2014).
7. J. J. McDonnell, The two water worlds hypothesis: ecohydrological separation of water between streams and trees? *Wiley Interdiscip. Rev. Water* (2014), doi:10.1002/wat2.1027.
8. M. Stieglitz, An approach to understanding hydrologic connectivity on the hillslope and the implications for nutrient transport. *Global Biogeochem. Cycles.* **17** (2003), , doi:10.1029/2003GB002041.
9. M. Weiler, J. J. McDonnell, Conceptualizing lateral preferential flow and flow networks and simulating the effects on gauged and ungauged hillslopes. *Water Resour. Res.* **43** (2007), doi:10.1029/2006WR004867.
10. J. R. Brooks, H. R. Barnard, R. Coulombe, J. J. McDonnell, Ecohydrologic separation of water between trees and streams in a Mediterranean climate. *Nat. Geosci.* **3**, 100–104 (2009).
11. G. R. Goldsmith *et al.*, Stable isotopes reveal linkages among ecohydrological processes in a seasonally dry tropical montane cloud forest. *Ecohydrology.* **5**, 779–790 (2012).
12. F. M. Phillips, Hydrology: Soil-water bypass. *Nat. Geosci.* **3**, 77–78 (2010).
13. G. Dongmann, H. W. Nürnberg, H. Fürstel, K. Wagener, On the enrichment of H 2 18 O in the leaves of transpiring plants. *Radiat. Environ. Biophys.* **11**, 41–52 (1974).
14. H. Craig, L. I. Gordon, in *Stable Isotopes in Oceanographic Studies and Paleotemperatures*, E. Tongioli, Ed. (Consiglio Nazionale Delle Ricerche Laboratorio Di Geologica Nucleare, Pisa, Italy, 1965), pp. 9–130.
15. J. J. Gibson, T. W. D. Edwards, Regional water balance trends and evaporation--transpiration partitioning from a stable isotope survey of lakes in northern Canada. *Global Biogeochem. Cycles.* **16**, 10–11 (2002).
16. J. R. Brooks *et al.*, Stable isotope estimates of evaporation : inflow and water residence time for lakes across the United States as a tool for national lake water quality assessments. *Limnol. Oceanogr.* **59**, 2150–2165 (2014).

17. X. F. Wang, D. Yakir, Using stable isotopes of water in evapotranspiration studies. *Hydrol. Process.* **14**, 1407–1421 (2000).
18. E. A. Yezpey *et al.*, Dynamics of transpiration and evaporation following a moisture pulse in semiarid grassland: a chamber-based isotope method for partitioning flux components. *Agric. For. Meteorol.* **132**, 359–376 (2005).
19. S. P. Good *et al.*,  $\delta^2\text{H}$  isotopic flux partitioning of evapotranspiration over a grass field following a water pulse and subsequent dry down. *Water Resour. Res.* **50**, 1410–1432 (2014).
20. A. M. J. Coenders-Gerrits *et al.*, Uncertainties in transpiration estimates. *Nature.* **506**, E1–2 (2014).
21. D. R. Schlaepfer *et al.*, Terrestrial water fluxes dominated by transpiration: Comment. *Ecosphere.* **5**, 1–9 (2014).
22. Materials and methods are available as supporting material on Science online.
23. S. P. Good, D. Noone, N. Kurita, M. Benetti, G. J. Bowen, D/H Isotope Ratios in the global hydrologic cycle (in press). *Geophys. Res. Lett.*
24. J. Worden *et al.*, Profiles of  $\text{CH}_4$ ,  $\text{HDO}$ ,  $\text{H}_2\text{O}$ , and  $\text{N}_2\text{O}$  with improved lower tropospheric vertical resolution from Aura TES radiances. *Atmos. Meas. Tech.* **5**, 397–411 (2012).
25. G. J. Bowen, J. Revenaugh, Interpolating the isotopic composition of modern meteoric precipitation. *Water Resour. Res.* **39**, 1–13 (2003).
26. S. P. Good, K. Soderberg, L. Wang, K. K. Caylor, Uncertainties in the assessment of the isotopic composition of surface fluxes: A direct comparison of techniques using laser-based water vapor isotope analyzers. *J. Geophys. Res.* **117**, D15301 (2012).
27. D. Wang, G. Wang, E. N. Anagnostou, Evaluation of canopy interception schemes in land surface models. *J. Hydrol.* **347**, 308–318 (2007).
28. R. F. Adler *et al.*, The Version-2 Global Precipitation Climatology Project (GPCP) Monthly Precipitation Analysis (1979–Present). *J. Hydrometeorol.* **4** (2003), pp. 1147–1167.
29. L. Wang-Erlandsson, R. J. Van Der Ent, L. J. Gordon, H. H. G. Savenije, Contrasting roles of interception and transpiration in the hydrological cycle – Part 1 : Temporal characteristics over land. *Earth Syst. Dyn.* **5**, 441–469 (2014).
30. I. Heidbüchel, P. A. Troch, S. W. Lyon, M. Weiler, The master transit time distribution of variable flow systems. *Water Resour. Res.* **48**, W06520 (2012).
31. M. Majoube, Fractionnement en oxygene 18 et en deuterium entre leau et sa vapeur. *J. Chim. Phys.* **68**, 1423–1436 (1971).
32. J. Horita, K. Rozanski, S. Cohen, Isotope effects in the evaporation of water: a status report of the Craig-Gordon model. *Isotopes Environ. Health Stud.* **44**, 23–49 (2008).
33. L. Merlivat, J. Jouzel, Global climatic interpretation of the deuterium-oxygen 18 relationship for precipitation. *J. Geophys. Res.* **84**, 5029–5033 (1979).

34. L. Yu, R. A. Weller, Objectively analyzed air-sea heat fluxes for the global ice-free oceans (1981-2005). *Bull. Am. Meteorol. Soc.* **88**, 527–539 (2007).
35. M. M. Rienecker *et al.*, MERRA: NASA's Modern-Era Retrospective Analysis for Research and Applications. *J. Clim.* **24**, 3624–3648 (2011).
36. G. D. Farquhar, L. A. Cernusak, On the isotopic composition of leaf water in the non-steady state. *Funct. Plant Biol.* **32**, 293–303 (2005).
37. G. J. Bowen, C. D. Kennedy, Z. Liu, J. Stalker, Water balance model for mean annual hydrogen and oxygen isotope distributions in surface waters of the contiguous United States. *J. Geophys. Res.* **116**, 1–14 (2011).

**Acknowledgments:** This project was funded by the NSF Macrosystems Biology program, Grant EF-01241286, and the Department of Defense. DN acknowledges the support of the NSF Climate and Large Scale Dynamic program as part of a Faculty Early Career Development award (AGS-0955841). The support and resources from the Center for High Performance Computing at the University of Utah is also gratefully acknowledged. Bulk flux data used in this study is available online from NASA (<http://precip.gsfc.nasa.gov/>, <http://gmao.gsfc.nasa.gov/merra/>) and the Woods Hole Oceanographic Institute (<http://oaflux.whoi.edu/>). Global surface vapor isotope data is available as supplementary information in ref (23). Model code and input data files used in this study are available at <http://waterisotopes.org>.



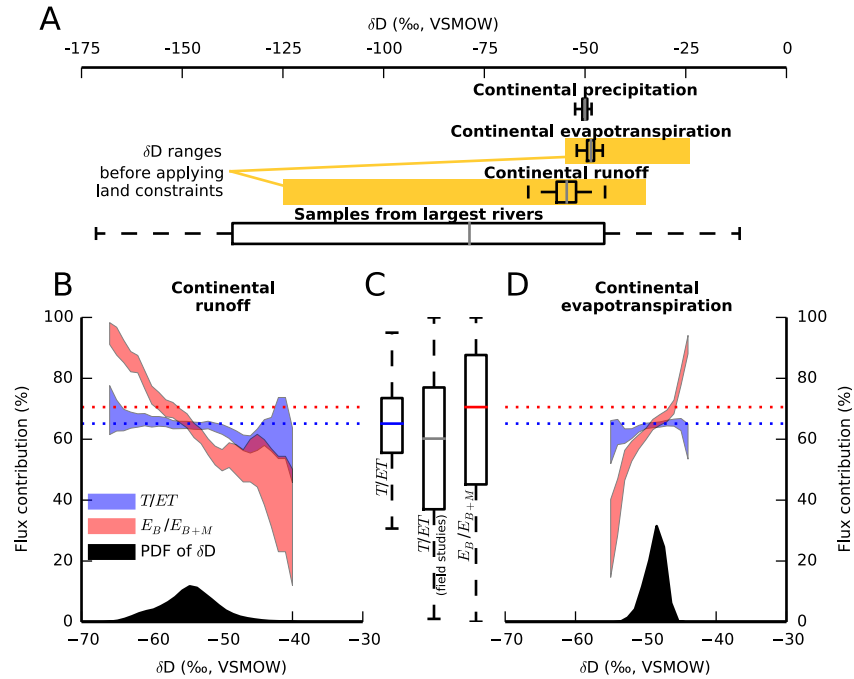


**Fig. 1. Continental hydrologic partitioning constrained by the global D/H ratios: (A)** Estimated global precipitation, evapotranspiration and runoff  $\delta D$  values compared with values from 23 of the 200 largest rivers (23). Boxplots depict median, 25<sup>th</sup>, and 75<sup>th</sup> percentiles of simulations, while yellow boxes depict the range based only on an ocean and atmosphere mass balance. Isotope values are reported in  $\delta$  notation where,  $\delta D = R/R_{VSMOW} - 1$ , with  $R$  the D/H isotope ratio. **(B)** Relationship between runoff  $\delta D$  and the transpired fraction of evapotranspiration,  $T/ET$  (blue), the fraction of evaporation from soils,  $E_B/E_{B+M}$  (red), and a kernel density estimate, PDF of  $\delta D$ , of the distribution global runoff (black). Red and blue shaded areas show mean values, smoothed with a 5‰ moving window,  $\pm$  two standard errors and dotted lines show median percentages of across all simulations. **(C)** Boxplot of  $T/ET$  from this study,  $T/ET$  from field studies, and  $E_B/E_{B+M}$  from this study. **(D)** The same as **(B)** for continental evapotranspiration  $\delta D$  values.

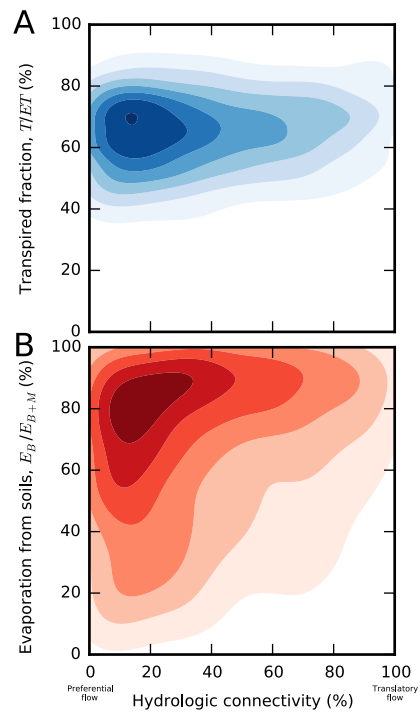


**Fig. 2. Relationship between hydrologic connectivity and hydrologic partitioning:** Bivariate kernel density plot shading of distribution of results from Monte Carlo simulations of D/H ratios in the continental water cycle, with darker areas more likely. (A) The transpired fraction of total evapotranspiration,  $T/ET$ , and (B) the fraction of soil and surface water evaporation that occurs from soils,  $E_B/E_{B+M}$ .

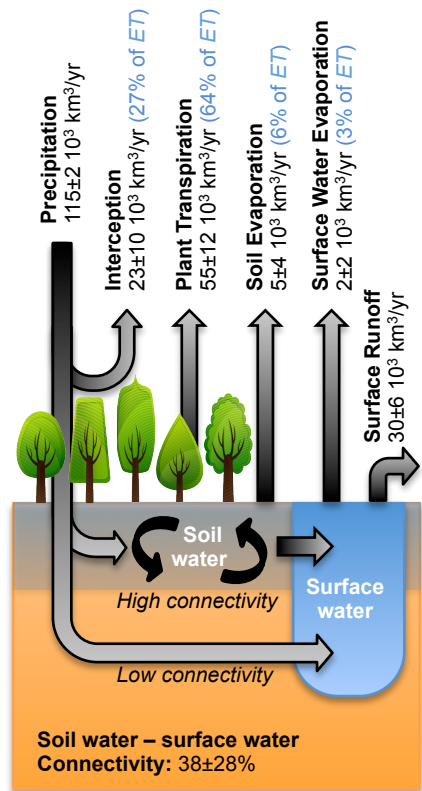


**Fig. 3. Partitioned continental hydrologic fluxes:** Terrestrial precipitation (annual mean  $\pm 1$  standard deviation) not intercepted by vegetation mixes into soils or flows into surface waters. Soil water is withdrawn by plant roots via transpiration, subjected to evaporation, and leaks into the surface water. Of the flux entering the surface waters, 38% is derived from the soils, with the remainder consistent with precipitation routed directly via preferential flow paths. Surface water that does not evaporate returns the ocean as runoff.

**Supplementary Materials:**

Materials and Methods

Figures S1 - S3

References (31–37)